Acidic Properties of Various Silica Catalysts Doped with Chromium for the Oxidative Dehydrogenation of Isobutane to Isobutene

Shigeru SUGIYAMA[1,2]*, Takuya EHIRO[3], Yoshihisa NITTA[3], Ai ITAGAKI[3], Keizo NAKAGAWA[1,2], Masahiro KATOH[1], Yuuki KATOU[4], Shuji AKIHARA[4], Toshiya YASUKAWA[4], Wataru NINOMIYA[4]

[1]*Department of Advanced Materials, Institute of Technology and Science, The University of Tokushima, Minamijosanjima, Tokushima-shi, Tokushima 770-8506, Japan*

[2]*Department of Resource Circulation Engineering, Center for Frontier Research of Engineering, The University of Tokushima, Minamijosanjima, Tokushima-shi, Tokushima 770-8506, Japan*

[3]*Department of Chemical Science and Technology, The University of Tokushima, Minamijosanjima, Tokushima-shi, Tokushima 770-8506, Japan*

[4]*Otake Research Laboratories, Mitsubishi Rayon Co. Ltd., 20-1, Miyuki-cho, Otake-shi, Hiroshima 739-0693, Japan*

***Keywords*:** Oxidative Dehydrogenation, Isobutane, Isobutene, FSM-16, Chromium-doping

Abstract

Although previous researchers have found that FSM-16 (#16 Folded Sheet Mesoporous material) doped with chromium and related Cr-doped silica catalysts has shown great activity for the oxidative dehydrogenation of isobutane to isobutene, information on the nature of these catalysts is insufficient. For this study, three types of Cr-doped silica catalysts were prepared by applying the template ion exchange method. CrOx/FSM-16 and CrOx/SiO_2 were used as references. These catalysts were used for oxidative dehydrogenation, which was then characterized via various techniques. The most active catalyst was Cr-doped silica, which did not have the hexagonal structure that is characteristic of mesoporous FSM-16. Various characterizations showed that the catalytic activity of the Cr-species, stemmed from a weak acidic nature and a redox nature that originated from the combination of silicate and a Cr cation, as opposed to the hexagonal structure and strong acidic nature of FSM-16.

Introduction

The oxidative dehydrogenation of isobutane to isobutene has attracted attention since isobutene is a precursor for the production of methyl methacrylate (MMA) (Nagai, 2001; Kuroda, 2003) and methyl tertially butyl ether (MTBE) (Eldarsi and Douglas, 1998). The former is used for the production of acrylic resin while the latter is a high-octane-number gasoline additive. In our laboratory, magnesium vanadates, magnesium molybdates, and hydroxyapatites, all of which had shown suitable activity for the oxidative dehydrogenation of propane, have been employed for the oxidative dehydrogenation of isobutane, which resulted in a lower yield of isobutene of up to 2% (Furukawa *et al*., 2011) at reaction temperatures lower than 723 K. However, in our laboratory, FSM-16 doped with chromium and the related catalysts previously showed a suitable activity with a yield of isobutene that was greater than 8% at 723 K (Sugiyama *et al*., 2013a). These results were superior, or at least comparable to earlier results using various single and binary oxides, metal phosphates, heteropoly acid, mesoporous silica (MCM-41 and SBA-15) doped with vanadium, aluminum, or chromium, and a number of supported and unsupported transition metal oxides, for which the maximum yield of isobutene was 8－11% at reaction temperatures greater than 673 K (Crzybowska *et al*., 1998; Sulikowski *et al*., 2002; Takita *et al*., 2005a; Wang *et al*., 2009).

FSM-16 (#16 Folded Sheet Mesoporous material) was first prepared in 1993 (Inagaki *et al.,* 1993) and featured characteristics such as a hexagonal structure and rather strong acidic properties that would compare favorably to another typical mesoporous silica MCM-41 (#41 Mobil Composition of Matter) (Iwamoto *et al.*, 2003). Hydrothermal conditions are needed for the preparation of MCM-41 and the result is thermally unstable. In contrast, hydrothermal conditions are unnecessary for the preparation of FSM-16, which is, therefore, a thermally stable product (Sugiyama *et al*., 2010). Furthermore, various cations can be incorporated into FSM-16 using template ion exchange (TIE), in which the cations are exchanged with the Si^{4+} in FSM-16 (Sugiyama *et al*., 2010). TIE was first suggested for MCM-41 (Yonemitsu *et al*., 1997; Iwamoto *et al*., 2003). The catalytic activity for the dehydrogenation of propane on MCM-41 doped with Cr cation via TIE was previously reported (Wang *et al*., 2003; Takehira *et al*., 2004). The use of TIE was also confirmed for FSM-16 (Sugiyama *et al*., 2010). Although we previously reported the successful oxidative dehydrogenation of isobutane to isobutene on FSM-16 doped with chromium prepared using TIE and

Correspondence concerning this article should be addressed to
S. Sugiyama (E-mail address: sugiyama@chem.tokushima-u.ac.jp

related catalysts (Sugiyama *et al*., 2013a), investigation into the structural and acidic nature of those Cr-doped catalysts has been insufficient.

In the present study, therefore, the oxidative dehydrogenation of isobutane to isobutene was examined using catalysts that were prepared applying the TIE method for the doping of Cr^{3+} into FSM-16, followed by various characterizations such as XRD, XPS, TEM, N_2 adsorption-desorption isotherms, NH_3-TPD, and in-situ FT-IR using NH_3 as a probe molecule and Hammett indicators. As references, CrOx/FSM-16 and CrOx/SiO_2 were also employed in the present study.

1. Experimental

FSM-16 was prepared using a hydrated sodium silicate powder (Kishida Chemical Co. Ltd.; a molar ratio of SiO_2/Na_2O = 2.00) and cetyl trimethyl ammonium bromide (Wako Pure Chemical Industries, Ltd.; (CTA)Br), according to a procedure established by Inagaki *et al.* (1993, 1996). After the calcination of a hydrated sodium silicate powder (5.0 g) at 973 K for 6 h, the calcined solid was grinded, added to 50 mL of water, and then stirred for 3 h at room temperature. While the stirring, hydrated sodium silicate powder was converted to kanemite ($NaHSi_2O_5 \cdot 3H_2O$). The kanemite was separated using a centrifuge and was added to 100 mL of an aqueous solution consisting of (CTA)Br (0.01 mol) (Step 1). The solution was refluxed at 343 K for 3 h and then cooled to room temperature. The solution pH was adjusted to 8.5 using 2 M HCl and then stirred at 343 K for 18 h. The resultant solid was washed, filtered and dried at 373 K for 24 h to obtain a white solid (Step 2). FSM-16 was obtained after the calcination of the resultant solid at 823 K for 8 h. In the doping of the chromium species, two procedures were employed. First, $Cr(NO_3)_3 \cdot 9H_2O$ (Sigma-Aldrich Japan) was added together with (CTA)Br in Step 1 and the obtained catalyst was denoted as Cr*-FSM-16. Second, aqueous $Cr(NO_3)_3$ was added in Step 2 using the TIE method (Iwamoto *et al.*, 2003; Sugiyama *et al*., 2010), followed by separation using filtration with washing. The catalyst thus prepared was denoted as Cr-FSM-16. Chromium oxide catalysts supported on FSM-16 and SiO_2 (CAB-O-SIL, Cabot Co.) (denoted as CrOx/FSM-16 and CrOx/SiO_2, respectively) were prepared from impregnation using $Cr(NO_3)_3 \cdot 9H_2O$. The wet FSM-16, Cr*-FSM-16, Cr-FSM-16 and CrOx/FSM-16 were dried at 333 K for 24 h, roughly crushed and calcined at 823 K for 8 h, followed by sieving to 0.85 − 1.70 mm particles. This molding procedure is referred to as wet-treatment in the present paper. It should be noted that the employment of typical pressurization for the molding of FSM-16 and a related catalyst was not suitable due to the collapse of the hexagonal structure of FSM-16 (Sugiyama *et al*., 2013a, 2013b). For the molding of CrOx/SiO_2, typical pressurization was employed.

The catalysts were characterized by X-ray diffraction (XRD; RINT 2500X using monochromatized Cu Kα radiation, Rigaku Co.). The surface on some catalysts was analyzed via X-ray photoelectron spectroscopy (XPS; ESCA-1000AX, Shimadzu Corp.) using monochromatized Mg Kα radiation. The binding energies were corrected using 285 eV for C 1s as an internal standard. Transmission electron microscope (TEM) images of the catalysts were recorded with a JEM-2100F (JEOL Ltd.). N_2 adsorption-desorption isotherms were obtained using a BELSORP-18SP (Bel Japan Inc.). The loading of Cr in Cr-FSM-16 and in Cr*-FSM-16 was analyzed using inductively coupled plasma-atomic emission spectrometry (ICP-AES: Optima 3000, PerkinElmer Japan). A desorption of ammonia onto the catalysts was characterized by temperature-programmed desorption (NH_3-TPD; BELCAT-A-SP, Bel Japan Inc.) and *in-situ* infrared spectroscopy (*in-situ* NH_3-FT-IR; FTX3000MX, Bio Rad Inc., resolution of $4cm^{-1}$). In NH_3-TPD, a catalyst (50 mg) was heated to 773 K at 10 K/min under a He flow (50.0 sccm, standard cubic centimeter per min). This temperature was held for 1 h under the He flow. Then the catalyst was cooled to 373 K under the He flow, and held at 373 K for 10 min. At this temperature, the catalyst was treated with 5% NH_3/He (50.0 sccm) for 30 min. After the treatment, the catalyst was again kept under a He flow (50.0 sccm) for 15 min. The catalyst then was heated from 373 to 773 K at 10 K/min under a He flow (30.0 sccm). The desorbed NH_3 from the catalyst during the final process was analyzed using a quadrupole mass spectrometer (OmniStar-s, Pfeiffer Vacuum GmbH). A fragment peak at m/e=16 was used to monitor the NH_3. The catalyst was also analyzed using *in-situ* NH_3-FT-IR. A catalyst disc 13 mm in diameter and approximately 8.5 mg in weight was degassed in the *in-situ* FI-IR cell (Katoh *et al*., 2012) at 723 K and 6.0×10^{-3} Pa for 1 h. Then the temperature was cooled to 323 K and IR was monitored at this temperature to obtain a standard spectra. The NH_3 gas (13.3 kPa) was then introduced into the cell at 323 K for 10 min. The excess NH_3 gas was degassed from the cell at 323 K to monitor the IR. The temperature was then increased to 423 K and held there for 10 min. The IR was again monitored. This process was repeated at temperatures of 523, 623 and 723 K. Temperature-programmed reaction (TPR) of the catalyst using H_2 was performed using BELCAT-A-SP (Bel Japan Inc.). For TPR, 5 vol% H_2/Ar was used as a reducing gas at a rate of 40 sccm. The heating rate was adjusted by 10 K/min from 323 to 1173 K. We used 50 mg of the catalyst and a quartz U-tube for the TPR measurement. The sample (50 mg) was pretreated in quartz U-tubes under an Ar gas flow (50 sccm) at 773 K for 1 h. Prior to measuring the H_2 consumption by TCD, a 13X

molecular sieve was used to trap the H_2O. The acid strength of the catalysts was analyzed using a toluene (Wako Pure Chemical Industries, Ltd.) solution of Hammett indicators such as methyl red (pKa = 4.8; Kanto Chemical Co., Inc.), 4-phenylazo-1-naphthylamine hydrochloride (pKa = 4.0; Wako Pure Chemical Industries, Ltd.), methyl yellow (pKa = 3.3; Kanto Chemical Co., Inc.), 4-phenylazodiphenylamine (pKa = 1.5; Kanto Chemical Co., Inc.), and dicinnamal-acetone (pKa = -3.0; Tokyo Chemical Industry Co., Ltd.) (Hawke and Steigman, 1954; Ito, 1986). According to the standard method (Ito, 1986), the indicator showing the lowest pKa (pKa = -3.0; dicinnamalacetone) was used first. Then, 4-phenylazodiphenylamine (pKa = 1.5), methyl yellow (pKa = 3.3), 4-phenylazo-1-naphthylamine hydro-chloride (pKa = 4.0), and methyl red (pKa = 4.8) were used in turn. Since all of the catalysts showed color changes when using methyl red, further examination was not conducted. A Johnson procedure using a titration of n-butylamine (Kanto Chemical Co., Inc.) was employed to estimate the acid amount of the catalyst (Johnson, 1955; Matsuzaki *et al.,* 1969).

The catalytic reactions were performed in a fixed-bed continuous reactor. In all experiments, the catalysts (0.85 − 1.70 mm) were heated to the reaction temperature under a continuous flow of helium (30 mL/min), then pretreated at the same temperature under an oxygen flow (25 mL/min) for 1 h. The values for the weight of the catalysts and the flow rate of the reactant gas were 0.25 g and 15 mL/min for FSM-16-related catalysts and 0.50 g and 30 mL/min for $CrOx/SiO_2$, respectively, in order to maintain the same space time. Other reaction conditions were as follows: $P(isoC_4H_{10})$ = 14.4 kPa, $P(O_2)$ = 12.3 kPa, and T = 723 K. No homogeneous reaction of isobutane was observed under the present reaction conditions. The reaction was monitored using an online Shimadzu GC-8APT gas chromatograph with a TC detector. Two columns, Hayesep R (2 m × 3 mm) and molecular sieve 5A (0.2 m × 3 mm), were used in the analyses. The conversion of isobutane was calculated from the products and from the isobutane introduced into the feedstream. The selectivities were calculated from the conversion of isobutane to each product on a carbon basis. The carbon mass balance was 100 ± 5%.

2. Results and Discussion

2.1 Oxidative dehydrogenation of isobutane on Cr-doped silica catalysts

The catalytic activity for the oxidative dehydrogenation of isobutane on FSM-16, Cr-FSM-16, Cr*-FSM-16, CrOx/FSM-16 and $CrOx/SiO_2$ is listed in **Table 1**. It should be noted that with the exception of $CrOx/SiO_2$, these catalysts were molded by wet treatment. Previous studies have reported lower catalytic activity for oxidative dehydrogenation and dehydration on FSM-16-related catalysts when pressurization was employed in the molding (Sugiyama *et al*., 2013a, 2013b, respectively). Since the activity during 6 h on-stream was rather stable for all catalysts, the conversions of isobutane and oxygen, and the selectivities to isobutene, CO, CO_2 and others, along with the yield of isobutene at 6 h on-stream all are shown in Table 1.

Table 1 Catalytic activity for the oxidative dehydrogenation of isobutane on Cr-doped silica catalysts

Catalyst	Cr [wt.%]	Conversion [%]		Selectivity [%]				Yield [%]
		isoC4H10	O2	isoC4H8	CO	CO2	Others	isoC4H8
FSM-16	0	15.1	96	8.8	40.7	40.7	9.8	1.3
Cr-FSM-16	0.3	16.9	93	11.7	39.1	42.4	6.8	2.0
Cr*-FSM-16	6.2	18.8	83	43.8	15.0	34.4	6.8	8.3
Cr*-FSM-16	9.1	21.4	91	40.1	16.0	40.8	3.1	8.6
CrOx/FSM-16	5.0	22.8	100	23.9	17.2	55.6	3.3	5.5
CrOx/FSM-16	9.1	22.1	100	27.4	14.4	55.1	3.1	6.0
CrOx/SiO2	5.0	21.2	100	23.4	14.6	58.4	3.6	5.0

As expected from our previous paper (Sugiyama *et al*., 2013a), the order of the yield of isobutene from the Cr-doped, but not from a Cr-supported, catalyst was Cr*-FSM-16>Cr-FSM-16>FSM-16. When using the TIE method, the Cr-loading into FSM-16 was strictly limited. Therefore, in Cr*-FSM-16, further Cr was added to reach 9.1 wt% of Cr, which showed the highest yield of isobutene (8.6%) in our runs. The highest selectivity to isobutene was observed with 6.2 wt% Cr*-FSM-16. The results for the selectivity and the yield of isobutene with Cr*-FSM-16 were evidently greater than those with Cr-FSM-16, CrOx/FSM-16 or $CrOx/SiO_2$, regardless of Cr loading. This indicated that the catalytic activity may not be dependent on the loading of Cr and Cr species, but, rather, on the structural or acidic influence of Cr*-FSM-16 itself.

2.2 Structural properties of Cr-doped silica catalysts

Figure 1 shows the XRD patterns of FSM-16, 0.3 wt.% Cr-FSM-16, and 5.0 wt.% CrOx/FSM-16. The XRD patterns of these catalysts showed three diffraction peaks characteristic to the hexagonal structure of FSM-16 at diffraction angles (2θ) of between 2.0 and 5.0 degrees (**Figure 1 (A)**), which were assigned as diffraction peaks due to the (100), (110) and (200) planes of FSM-16 (Inagaki *et al*., 1993). This seemed to be reasonable since those catalysts were prepared using either FSM-16 or its precursor. It was also reasonable that these three diffraction peaks were not detected from 5.0 wt.% $CrOx/SiO_2$.

It is noteworthy that the three peaks were also not detected from 6.2 wt.% Cr*-FSM-16, indicating that the simultaneous addition of $Cr(NO_3)_3 \cdot 9H_2O$ and (CTA)Br in Step 1 in the preparation resulted in the formation of amorphous silica rather than in a hexagonal structure. From the most selective catalyst, 6.2 wt% Cr*FSM-16, XRD peaks due to Cr_2O_3 were detected (JCPDS 381479), indicating the presence of a lower degree of

dispersion for the oxide (**Figure 1 (B)**). From FSM-16, 0.3 wt.% Cr-FSM-16, and 5.0 wt.% CrOx/FSM-16, XRD peaks due to crystalline SiO_2 (JCPDS 501432) were also detected (Figure 1 (B)). Since the catalytic activity on CrOx/FSM-16 and CrOx/SiO_2 was evidently lower than that on Cr*-FSM-16, the formation of Cr_2O_3 did not directly contribute to the activity of Cr*-FSM-16.

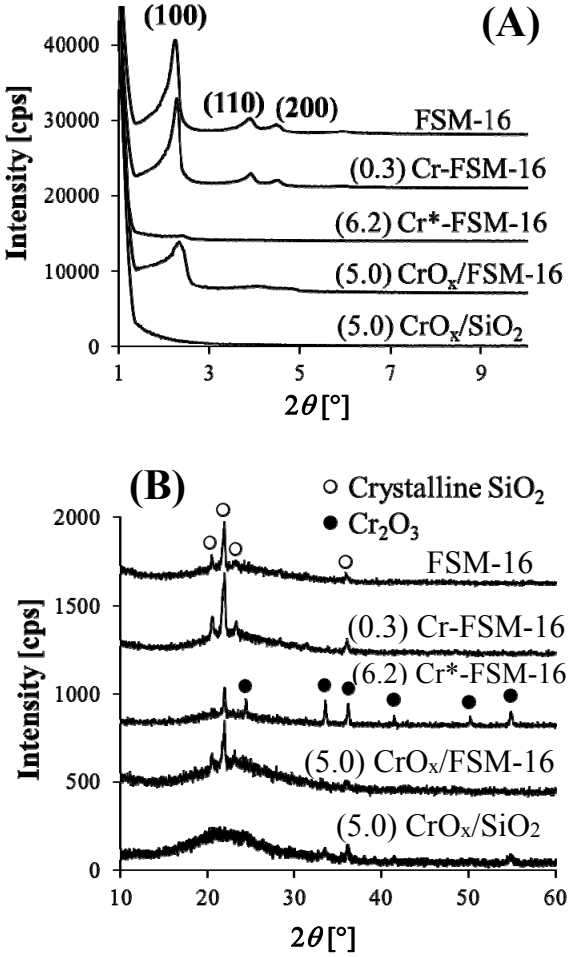

Fig. 1 XRD patterns of FSM-16, 0.3 wt.% Cr-FSM-16, 6.2 wt.% Cr*-FSM-16, 5.0 wt.% CrOx/FSM-16 and 5.0 wt.% CrOx/SiO_2 detected from (A) lower and (B) higher diffraction angles

In order to examine the effect of the presence and absence of the hexagonal structure, FSM-16, 0.3 wt% Cr-FSM-16 and 6.2 wt% Cr*-FSM-16 were analyzed using TEM (**Figures 2 (A)－(D)**, respectively). With FSM-16 and 0.3 wt.% Cr-FSM-16, a hexagonal structure was evident, as shown in Figures 2 (A) and (B), respectively. However, such a structure was not detected with 6.2 wt.% Cr*-FSM-16, while shapes such as hose and needle crystals, probably due to Cr_2O_3, were detected (Figures 2 (C)－(D)). These results were also supported by the corresponding XRD data (Figure 1).

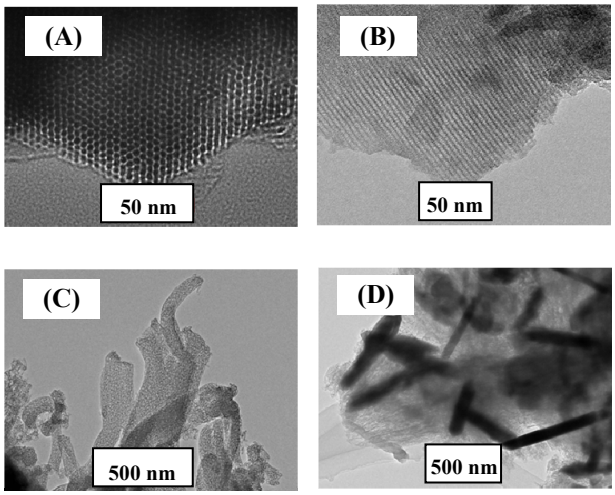

Fig. 2 TEM images of FSM-16 (A), 0.3 wt.% Cr-FSM-16 (B) and 6.2 wt.% Cr*-FSM-16 (C and D)

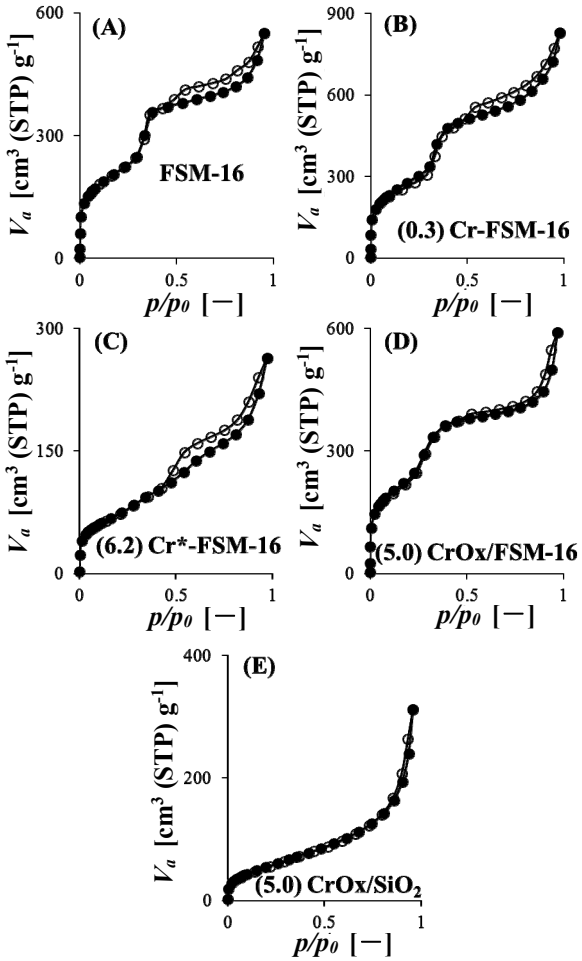

Fig. 3 N_2 adsorption-desorption isotherms obtained from (A) FSM-16, (B) 0.3 wt.% Cr-FSM-16, (C) 6.2 wt.% Cr*-FSM-16, (D) 5.0 wt.% CrOx/FSM-16 and (E) 5.0 wt.% CrOx/SiO_2

In **Figures 3 (A)-(E)**, N_2 adsorption-desorption isotherms obtained from FSM-16, 0.3 wt.% Cr-FSM-16, 6.2 wt.% Cr*-FSM-16, 5.0 wt.% CrOx/FSM-16 and 5.0 wt.% CrOx/SiO_2, respectively, are shown. The isotherms that are characteristic to mesoporous silica were detected from FSM-16 (A), 0.3 wt% Cr-FSM-16 (B) and 5.0 wt% and CrOx/FSM-16 (D) in contrast with those obtained from 6.2 wt% Cr*-FSM-16 (C) and 5.0 wt% CrOx/SiO_2 (E). Furthermore, the amounts of N_2 adsorbed on the former three catalysts were evidently greater than those adsorbed on the latter two catalysts. In **Table 2**, the pore sizes, pore volumes and specific surface areas of those catalysts are summarized. According to the results shown in Figures 3 (A)-(E) and Table 2, those five catalysts were classified into one of two groups: 1) a greater specific surface area together with mesoporous structure; or 2) a smaller specific surface area without a mesoporous structure. It should be noted that the most active catalyst among these five was the 6.2 wt.% Cr*-FSM-16, which showed a smaller specific surface area without a mesoporous structure. This indicates that the acidic properties of these five catalysts may have contributed to the catalytic activity.

Table 2 Pore size, pore volume and specific surface area obtained from N_2 adsorption-desorption isotherms

Catalyst	Cr [wt%]	Pore size [nm]	Pore volume [cm^3/g]	Surface area [m^2/g]
FSM-16	0	4.4	0.8	771
Cr-FSM-16	0.3	5.0	1.3	1019
Cr*-FSM-16	6.2	6.2	0.4	263
CrOx/FSM-16	5.0	4.4	0.9	833
CrOx/SiO2	5.0	9.1	0.5	211

2.3 Acidic properties of Cr-doped silica catalysts

The acidic nature of FSM-16 was carefully examined by Yamamoto *et al.* (1998) and the conclusion was that the active sites were weakly perturbed silanol groups and a trace amount of Al, which derived from the raw material, sodium silicate powder, which did not affect the acidic properties. They also reported that the greatest acid strength was pKa = -3.0. As shown in **Table 3**, the greatest acid strength of our FSM-16 was pKa = 1.5, while that (pKa = 4.8) of 6.2 wt% Cr*-FSM-16, which was the best catalyst employed in the present study, was the weakest acid among the catalysts employed.

Furthermore, the smallest acid amount was also detected from 6.2 wt.% Cr*-FSM-16 (**Figure 4**). As generally accepted (Ito, 1986), the distribution of acid amount is decreased with increasing acid strength (decreasing pKa value of the indicators). As shown in Figure 4 (A), a similar distribution behavior was observed using FSM-16, indicating that the estimation in the present study was reasonable particularly in using FSM-16, the color of which was white. Unfortunately, the color of Cr-doped catalysts was not white and it was rather difficult to strictly detect the color change of Cr-doped catalysts by Hammett indicators. As shown in Figures 4 (B)-(E), from four Cr-doped catalysts, we could not detect an evident color change at pKa=4.0 using a Hammett indicator (4-phenylazo-1-naphthylamine hydrochloride). Also, the differences in acid amounts at pKa = 3.3 and 1.5 for 5.0 CrOx/FSM-16 and 5.0 CrOx/SiO_2 were small and in reverse order of the distribution of the acid amount that was detected.

Table 3 Acid strength estimated using Hammett indicator

Catalyst	Cr [wt%]	pKa				
		4.8	4.0	3.3	1.5	-3.0
FSM-16	0	+	+	+	+	−
Cr-FSM-16	0.3	+	+	+	+	−
Cr*-FSM-16	6.2	+	−	−	−	−
CrOx/FSM-16	5.0	+	−	+	+	−
CrOx/SiO2	5.0	+	−	+	+	−

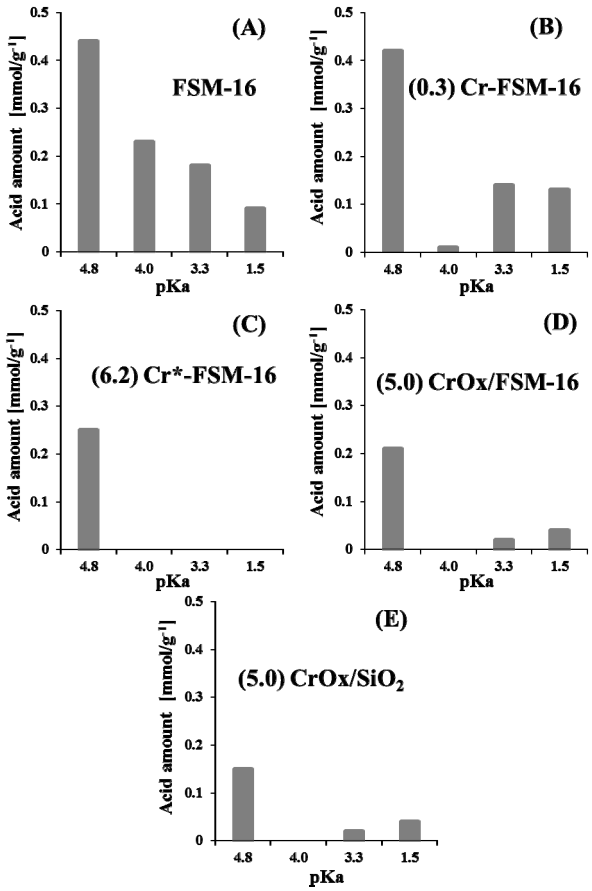

Fig. 4 Acid amount of (A) FSM-16, (B) 0.3 wt% Cr-FSM-16, (C) 6.2 wt% Cr*-FSM-16, (D) 5.0 wt% CrOx/FSM-16 and (E) 5.0 wt% CrOx/SiO_2.

Although the distribution of acid amount could not be strictly estimated, as shown in Figure 4, these five catalysts were classified into one of three groups. The first group included FSM-16 and 0.3 wt% Cr-FSM-16. The distributions of the acid amounts of FSM-16 and that of 0.3 wt% Cr-FSM-16 were similar, with the noted exception of those with a pKa = 4.0, and showed the greatest acid amount from among the five catalysts. It should be noted that the isobutene yield using 0.3 wt% Cr-FSM-16 was better than that using FSM-16, indicating that the lower acid amount may have resulted in better activity. The second group included 5.0 wt% CrOx/FSM-16 and 5.0 wt% CrOx/SiO_2. The distributions of the acid amounts for 5.0 wt% CrOx/FSM-16 and 5.0 wt% CrOx/SiO_2 were similar and were smaller than that of the first group. The yield of isobutene using the second group was better than that using the first group, again indicating that the lower acid amount may have resulted in better activity. The third group was made up of only 6.2 wt% Cr*-FSM-16. The acid amount of this catalyst was not detected at an acid strength lower than pKa = 4.0, and this catalyst showed the greatest yield of isobutene among these five catalysts. Therefore, it may be concluded that a lower acid amount results in better activity.

In order to clarify the difference between FSM-16, 0.3 wt% Cr-FSM-16, and 6.2 wt% Cr*-FSM-16, the adsorption-desorption behavior of NH_3 was examined using an *in-situ* FT-IR cell (Katoh *et al*., 2012) (**Figures 5 (A)－(C)**, respectively). IR peaks due to silanol were detected from these three catalysts prior to the adsorption of NH_3, at approximately 3,700 cm^{-1} ((a) in Figures 5 (A)－(C)) (Yamamoto *et al*., (1998)). After the adsorption of NH_3 at 323 K, broader peaks due to the adsorpted NH_3 at wave numbers lower than 3,700 cm^{-1} were detected from the catalysts while the intensity of the peaks was dependent on the catalysts ((b) in Figures 5 (A)－(C)). With an increase in the desorption temperatures from 423 to 723 K, at each 100 K, the intensity became weaker ((c)－(f) in Figures 5 (A)－(C)), while the complete desorption of NH_3 at a lower temperature was evident particularly from 6.2 wt% Cr*-FSM-16. Therefore, the acid strength of 6.2 wt% Cr*-FSM-16 was the weakest among the three catalysts, as shown in the results using the Hammett indicator (Table 3 and Figure 4). It is noteworthy that the NH_3 desorption behavior of FSM-16 was similar to that of 0.3 wt% Cr-FSM-16, but different from that from 6.2 wt% Cr*-FSM-16. As shown above, the former two catalysts, FSM-16 and 0.3 wt% Cr-FSM-16, possessed hexagonal structures while the latter one, 6.2 wt% Cr*-FSM-16, did not.

Unique NH_3 adsorption behavior was also detected using NH_3-TPD (**Figure 6**). Although NH_3-desorption peaks were not evident from either FSM-16 or 0.3 wt% Cr-FSM-16 together with Cr_2O_3, an amount of NH_3 was evident at temperatures between 373 and 573 K from 6.2 wt% Cr*-FSM-16. The ratio of peak areas for [FSM-16] : [0.3 wt% Cr-FSM-16] : [6.2 wt% Cr*-FSM-16] was 1 : 2.2 : 9.4. Particularly for the latter two catalysts, this indicated that the addition of a small amount of Cr into FSM-16 using the TIE method (0.3 wt% Cr-FSM-16) resulted in the effective formation of an acid site.

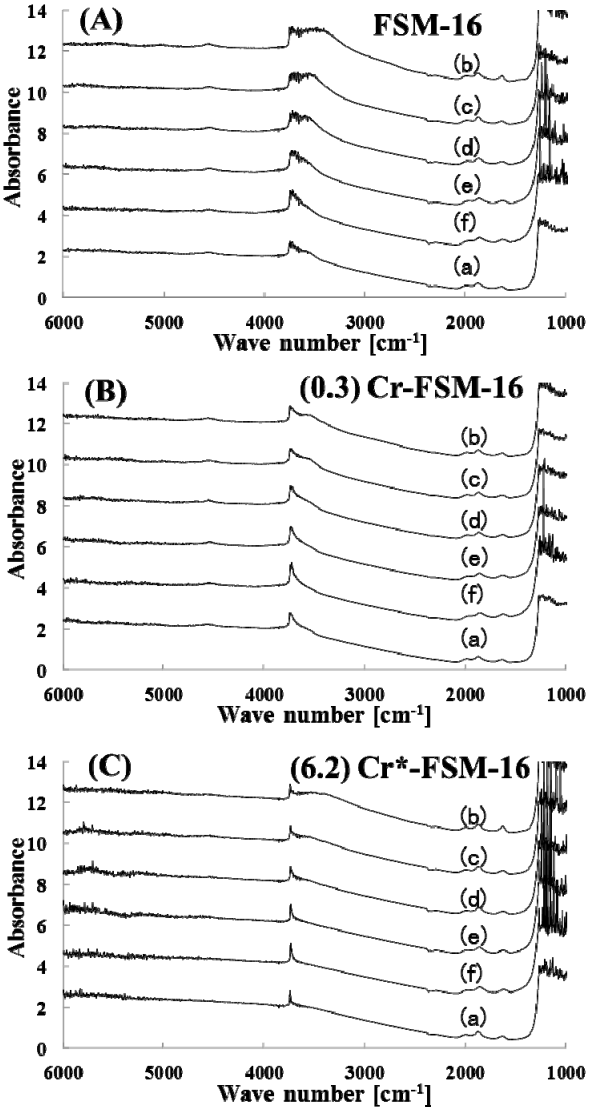

Fig. 5 *In-situ* NH_3-FT-IR of (A) FSM-16, (B) 0.3 wt% Cr-FSM-16 and (C) 6.2 wt% Cr*-FSM-16;
(a): before NH_3 adsorption at 323 K; (b): after NH_3 adsorption at 323 K; (c): after NH_3 desorption from (b) at 423 K; (d): after NH_3 desorption from (c) at 523 K; (e): after NH_3 desorption from (d) at 623 K; (f): after NH_3 desorption from (e) at 723 K

It is worth mentioning that the NH_3-TPD peak from FSM-16 was substantially weaker although the acidic nature would be undoubtedly great, as shown in the catalytic activity for the dehydration of ethanol to ethylene on FSM-16 (Sugiyama *et al*., 2010), indicating that NH_3-TPD may not be suitable for estimating the acidic properties of FSM-16 and related catalysts.

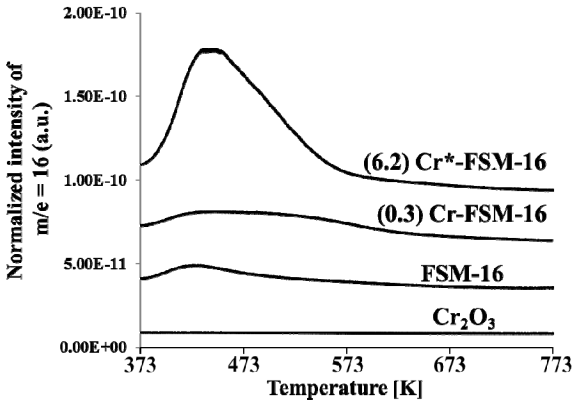

Fig. 6 NH_3-TPD of FSM-16, 0.3 wt% Cr-FSM-16, 6.2 wt% Cr*-FSM-16 and Cr_2O_3

2.4 Redox nature of chromium in Cr*-FSM-16 and the reaction mechanism

As shown above, 6.2 wt% Cr*-FSM-16 showed the greatest activity for the oxidative dehydrogenation of isobutane among the catalysts used in the present study. In order to estimate the redox nature of the Cr-species in the catalyst, XPS was employed. As shown in **Figure 7**, two Cr 2p signals due to Cr^{3+} and Cr^{6+} were detected from 6.2 wt% Cr*-FSM-16 before the reaction, while just one signal due to Cr^{3+} was detected after the reaction. However only one signal due to Cr^{3+} was detected from Cr-FSM-16 prepared using the TIE method (not shown). In Cr-FSM-16, the Cr-species was rather tightly fixed in the hexagonal structure since chromium was incorporated into the FSM-16 structure through an ion exchange between the silica in FSM-16 and chromium. In contrast, chromium may not have been so tightly fixed since Cr-species unbounded to silicate may have been present. Therefore, it is understandable that the Cr-species showed a redox nature and this Cr-species may have resulted in the greatest activity for the oxidative dehydrogenation of isobutane from among the catalysts examined in the present study.

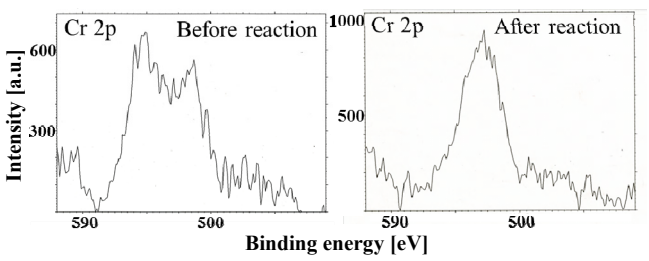

Fig. 7 XPS of Cr 2p from 6.2 wt% Cr*-FSM-16

Reducible Cr-species in 6.5 wt% Cr*-FSM-16 rather than those in 0.3 wt% Cr-FSM-16 were also confirmed using H_2-TPR (**Figure 8**). It was evident that the Cr-species in 6.5 wt% Cr*-FSM-16 was easily reduced at a temperature between 673 and 773 K, while those in 0.3 wt% Cr-FSM-16 showed no reducible properties in that temperature region. Since the reaction temperature in the present study was 723 K, it was evident that the reducible properties of the Cr-species in 6.5 wt% Cr*-FSM-16 contributed to the activity of the reaction.

Based on the present study, it is evident that the combination of weak acidic properties and the redox nature of the Cr-species contributed to the oxidative dehydrogenation of isobutane. Although it is generally accepted that the oxidative dehydrogenations of various alkanes mainly occur on basic catalysts (Kung, 1994), it also has been reported on acidic catalysts (Le Bars *et al*., 1992; Kung, 1994; Wang *et al*., 2003; Wang *et al*., 2009). Takita *et al* (2005b) have already reported the reaction mechanism for the oxidative dehydrogenation of isobutane on cerium phosphate, which possessed an acidic site and a cerium cation showing a redox nature of the catalyst. It should be noted that their catalyst system was similar to the present system. Therefore, based on the mechanism reported by Takita *et al*. (2005b), the following mechanism is tentatively proposed for the oxidative dehydrogenation of isobutane on Cr*-FSM-16. Isobutane is adsorbed onto the lattice oxygen and Cr^{6+} to form an isobuthylcarbenium cation and H^-, respectively. It should be noted that C-H activation of isobutane favorably proceeds due to the rather smaller bond energy of tertiary C-H (390 kJ/mol) compared with either primary C-H (420 kJ/mol) or secondary C-H (401 kJ/mol) (Kung, 1994), although it is generally accepted that C-H activation of aliphatic hydrocarbons is difficult. Isobutene is released from isobuthylcarbenium cations. The electron of H^- migrates to Cr^{6+} to form a reduced species of Cr^{6+}. The reduced species of Cr^{6+} is then oxidized to regenerate the original Cr^{6+}. Since Cr^{3+} was detected as the reduced species of Cr^{6+} from XPS, the formation step of the isobuthylcarbenium cation on Cr^{6+} should be repeated. Therefore, the redox nature of the Cr species, which was detected from XPS and TPR, seems to be the most important under the present conditions.

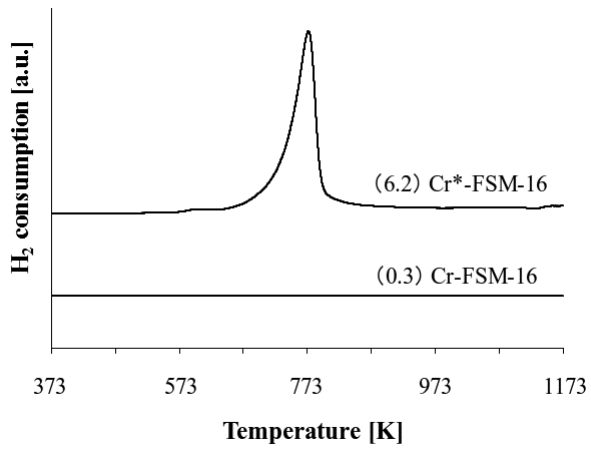

Fig. 8 H_2-TPR of 0.3 wt.% Cr-FSM-16 and 6.2 wt% Cr*-FSM-16

Conclusions

Among the five catalysts prepared in the present study, Cr*-FSM-16, which was prepared from a mixture of sodium silicate and $Cr(NO_3)_3 \cdot 9H_2O$, showed the greatest activity for the oxidative dehydrogenation of isobutane. From the results obtained using various forms of characterization, it was concluded that the Cr-species with weak acidic properties and a redox nature, both obtained from the combination of silicate with a Cr cation, showed better activity compared with FSM-16 with its hexagonal structure and its stronger acidic nature.

Acknowledgements

This work was funded by a Grant-in-Aid for Scientific Research (B) (KAKENHI 24360328) that was awarded to SS, for which we are grateful. The authors acknowledge Prof. Naonobu Katada (Tottori University, Japan) for his valuable suggestion on NH_3-TPD and Dr. Shinji Inagaki (Toyota Central Research and Development Laboratories, Japan) and Associate Prof. Takashi Yamamoto (The University of Tokushima, Japan) for their stimulating discussion on FSM-16.

Literature Cited

Crzybowska, B., J. Sloczynski, R. Grabowski, K. Wcislo, A. Kozlowska, J. Stoch and J. Zielinski; "Chromium Oxide/Alumina Catalysts in Oxidative Dehydrogenation of Isobutane," *J. Catal.*, **178**, 687—700 (1998)

Eldarsi, H. S. and P. L. Douglas; "Methyl-Tert-Butyl-Ester Catalytic Distillation Column: Part II: Optimization," *Chem. Eng. Res, Design*, **76**, 517—524 (1998)

Furukawa, Y., K. Nakagawa, K.-I. Sotowa, S. Sugiyama, Y.Katou and W. Ninomiya; "Effect of the Preparation Conditions of Magnesium Molybdates on the Oxidative Dehydrogenation of Isobutane," *24th Symposium on Chemical Engineering,* Gyeongju, Korea, PD-19 (2011)

Hawke, D. L. and J. Steigman; "Reactions of Some Lewis Acids with Series of Simple Basic Indicators in Aprotic Solvents," *Anal Chem.*, **26**, 1989—1992 (1954)

Inagaki, S., Y. Fukushima and K. Kuroda; "Synthesis of Highly Ordered Mesoporous Materials from a Layered Polysilicate," *J. Chem. Soc., Chem. Commun.*, 680-682 (1993)

Inagaki, S., A. Koiwai, N. Suzuki, Y. Fukushima and K. Kuroda; "Syntheses of Highly Ordered Mesoporous Materials, FSM-16, Derived from Kanemite," *Bull. Chem. Soc. Japan*., **69**, 1449—1457 (1996)

Iwamoto, M., Y. Tanaka, N. Sawamura and S. Namba; "Remarkable Effect of Pore Size on the Catalytic Activity of Mesoporous Silica for the Acetalization of Cyclohexanone with Methanol," *J. Am. Chem. Soc.,* **125**, 13032—13033 (2003)

Johnson, O.; "Acidity and Polymerization Activity of Solid Acid Catalysts," *J. Phys. Chem*. **59**, 827—831 (1955)

Katoh, M., R. Koide, K. Yamada, T. Yoshida and T. Horikawa; "IR Spectroscopic Analysis of Thermal Behavior of Adsorbed Water on Y-Type Zeolite," *Int. J. Mod. Phys. Conf. Ser.*, **6**, 437—442 (2012)

Kung, H. H.; "Oxidative Dehydrogenation of Light (C_2 to C_4) Alkanes," *Adv. Catal*., **40**, 1—38 (1994)

Kuroda, T.; "Development of Industrial Processes for MMA Production," *Catal. Catal.*, **45**, 366—371 (2003)

Le Bars, J., J. C. Vedrine, A. Auroux, S. Trautmann and M. Baerns; "Role of Surface Acidity on Vanadia/silica Catalysts Used in the Oxidative Dehydrogenation of Ethane," *Appl. Catal. A. Gen*., **88**, 179—195 (1992)

Matsuzaki, I., Y. Fukuda, T. Kobayashi, K. Kubo and K. Tanabe; "Titration Method Using n-Butylamine to Estimate Acid Amount on Solid Acids," *Shokubai*, **11**, 210—216 (1969)

Nagai, K.; "New Development of the Production of Methyl Methacrylate," *Appl. Catal. A, Gen.,* **221**, 367—377 (2001)

Ito, H.; "Catalytic Active Site on Solid Acidic Catalysts," Handbook for Catalyst Experiments in Sokubai Kouza, pp.170 — 172, Kodansha, Tokyo, Japan (1986)

Sugiyama, S., Y. Kato, T. Wada, S. Ogawa, K. Nakagawa and K.-I. Sotowa; "Ethanol Conversion on MCM-41 and FSM-16, and on Ni-Doped MCM-41 and FSM-16 Prepared without Hydrothermal Conditions," *Top. Catal.*, **53**, 550—554 (2010)

Sugiyama, S., Y. Nitta, Y. Furukawa, A. Itagaki, T. Ehiro, K. Nakagawa, M. Katoh, Y. Katou, S. Akihara and W. Ninomiya; "Oxidative Dehydrogenation of Isobutane to Isobutene on FSM-16 Doped with Cr and Related Catalysts," *J. Chem. Chem. Eng*., **7**, 1014—1020 (2013a)

Sugiyama, S., Y. Okada, Y. Kosaka, K. Nakagawa, M. Katoh, Y. Katou, S. Akihara, T. Yasukawa and W. Ninomiya; "The Catalytic Conversion of 1,2-Propandiol to Propanal on FSM-16 Molded by Wet-Treatment and Pressurization," *J. Chem. Eng. Japan*., **46**, 620—624 (2013b)

Sulikowski, B., Z. Olejniczak, E. Wloch, J. Rakoczy, R. X. Valenzuela and V. C. Corberan; "Oxidative Dehydrogenation of Isobutane on MCM-41 Mesoporous Molecular Sieves," *Appl. Catal. A. Gen*., **232**, 189—202 (2002)

Takehira, K., Y. Ohishi, T. Shishido, T. Kawabata, K. Takaki, Q. Zhang and Y. Wang; "Behavior of Active Sites on Cr-MCM-41 Catalysts during the Dehydrogenation of Propane with CO_2," *J. Catal.*, **224**, 404—416 (2004)

Takita, Y., K. Kikutani, C. Xia, H. Takami and K. Nagaoka; "Oxidation of Isobutane over Complex Oxides Containing V, Nb, Ta, and Mo under Aerobic and Anaerobic Reaction Conditions," *Appl. Catal. A. Gen*., **283**, 209—216 (2005a)

Takita, Y., X. Qing, A. Takami, H. Nishiguchi and K. Nagaoka; "Oxidative Dehydrogenation of Isobutane III. Reaction Mechanism over $CePO_4$ Catalyst," *Appl. Catal. A. Gen*., **296**, 63—69 (2005b)

Wang, G., L. Zhang, J. Deng, H. Dai, H. He and C. T. Au; "Preparation, Characterization, and Catalytic Activity of Chromia Supported on SBA-15 for the Oxidative Dehydrogenation of Isobutane," *Appl. Catal. A, Gen*., **355**, 192—201 (2009)

Wang, Y., Y. Ohishi, T. Shishido, Q. Zhang, W. Yang, Q. Guo, H. Wan and K. Takehira; "Characterizations and Catalytic Properties of Cr-MCM-41 Prepared by Direct Hydrothermal Synthesis and Template-ion Exchange," *J. Catal*., **220**, 347—357 (2003)

Yamamoto, T., T. Tanaka, T. Funabiki and S. Yoshida; "Acidic Property of FSM-16," *J. Phys. Chem. B*, **102**, 5830—5839 (1998)

Yonemitsu, M., Y. Tanaka and M. Iwamoto; "Metal Ion-Planted MCM-41. 1. Planting of Manganese (II) Ion into MCM-41 by a Newly Developed Template-Ion Exchange Method," *Chem. Mater.*, **9**, 2679—2681 (1997)